

Thermovoltage and heat dissipation in a triangle quantum dot junction

Ahmad Ahmadi Fouladi^{1,*} and Javad Vahedi^{2,1,†}

¹*Department of Physics, Sari Branch, Islamic Azad University, Sari 48164-194, Iran.*

²*Department of Physics and Earth Sciences, Jacobs University Bremen, Bremen 28759, Germany.*

(Dated: June 8, 2022)

We numerically investigate the thermoelectric properties of a triangle quantum dot connected to metallic electrodes using the non-equilibrium Green's function method in the Anderson model. Exploiting the equation of motion method in the Coulomb-blockade regime, the thermovoltage, thermocurrent and heat dissipation are calculated. Results show that the thermovoltage and thermocurrent have nonlinear behavior, and the magnitude and sign of them can be controlled with site energy and coupling strength of quantum dots. Moreover, we find that the heat current is nonlinear and asymmetric respect to the sign of bias voltage for all of the site energies of quantum dots. Analyses show that the heat current can be positive or negative for all of the site energies and becomes zero for the nonzero voltages. These results can be useful to determine the performance of the nanoscale electronic devices to control the heat dissipations.

I. INTRODUCTION

The thermoelectric properties of quantum dots (QDs) have attracted the attention of both theoretical and experimental researchers in recent years¹⁻¹⁷. Exploiting nanostructures such as QDs and organic molecules placed between metallic electrodes show high-efficiency energy conversion devices in the nonlinear regime¹⁸⁻²⁸. Accordingly, studying the thermoelectric properties of nanoscale systems provide a deeper insight into the nature and characteristics of the electron and heat transfer process.

Heat-to-electric converters operate through the Seebeck effect²⁹. The Seebeck effect arises when either electric and thermal forces act simultaneously on electron transmission through the desired system. When a temperature difference occurs along the system in the absence of bias voltage application, a thermovoltage V_{th} arises and in this case the electric current is zero. As a result, the formation of V_{th} implies the conversion of energy. In 1993, Staring et al. reported an interesting behavior of V_{th} in a QD in the presence of Coulomb-blockade³⁰. Their observations showed that V_{th} increases with the application of temperature bias, which is in agreement with the Seebeck effect. Moreover, at higher temperature biases, V_{th} decreases and then becomes zero for a non-zero temperature difference, and eventually its sign changes. Svensson, et al. also studied the nonlinear properties of temperature voltage in nanowires and obtained a similar result³¹.

The cause of this nonlinear behavior is attributed to the renormalization of energy levels by temperature; Because the accumulated charge depends on the applied temperature gradient. Unlike the current caused by the application of voltage, which has a definite sign for voltages greater than zero, by applying a temperature gradient, the heat current can be positive or negative, depending on the sign of the heat power. For electron-like charge carriers, it is a positive and for hole-like carriers, it is a negative¹⁸. However, in the linear response regime, the heat power is constant and the above reason

is not sufficient to change the heat flow sign. Therefore, a strong and negative differential heat conduction is needed to change the flow from positive to negative values¹⁸. It is interesting that by increasing the temperature of the electrodes, the heat flow through the QD may be zero. Notably, this is a completely nonlinear thermoelectric effect and bears no resemblance to voltage or linear thermoelectric regime.

Considering the effect of Coulomb-blockade in low temperature physics is important for nanometer systems^{32,33}. The effect of Coulomb interaction occurs when the energy of the electron-electron interaction becomes appreciable compare to the other energies scale of the model, such as the energies levels broadening and the temperature. Because electrons carry energy in the tunneling process, Coulomb-blockade can have a significant effect on heat conduction^{34,35}. In this paper, combining the non-equilibrium Green function and the equation of motion methods, we study thermovoltage, thermocurrent, and heat dissipation in a triangle QD attached to metallic electrodes, see Fig. 1 for a sketch, in the presence of electron-electron interaction.

The rest of the paper is organized as follows. In Sec. II, we first introduce the model and then give a detailed analytical derivation of transport properties with the combination of non-equilibrium Green's function and equations of motions. In Sec. III, we present numerical results and their interpretations. Conclusion are summarized in Sec. IV.

II. MODEL AND FORMALISM

Here we study three QDs setup in as a triangle structure attached to metallic leads. The leads are connected to the QD₀, as shown in Fig. 1. Moreover, we consider a bias voltage and temperature gradient between the two leads. The total Hamiltonian describing the device is given by

$$\mathcal{H} = \mathcal{H}_L + \mathcal{H}_{L-dot} + \mathcal{H}_{dot} + \mathcal{H}_R + \mathcal{H}_{R-dot}, \quad (1)$$

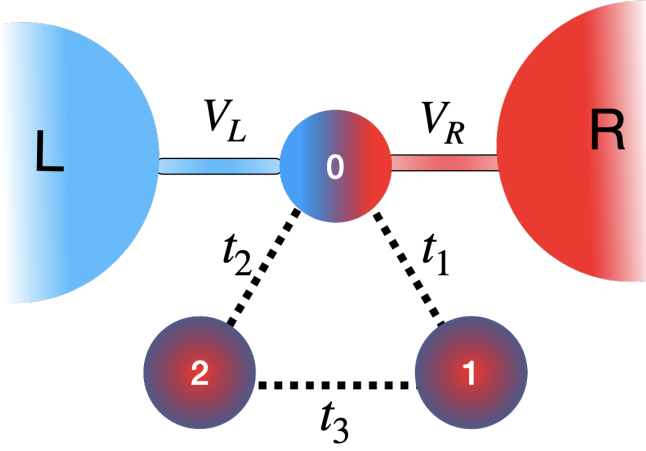


FIG. 1. (color online) Cartoon showing the model with a triangular quantum dot attached to semi-infinite metallic leads to which both a voltage ΔV difference and a temperature difference ΔT are applied.

where $\mathcal{H}_{L/R} = \sum_{k\sigma} \epsilon_{k\sigma} c_{k\sigma}^\dagger c_{k\sigma}$ corresponds to the left (right) metallic lead. $c_{k\sigma}^\dagger$ ($c_{k\sigma}$) creates (annihilates) an electron at state (k, σ) in the lead $\alpha = L/R$. The term $\mathcal{H}_{\alpha-dot} = \sum_{k\alpha\sigma} (\mathcal{V}_{k\alpha\sigma} c_{k\alpha\sigma}^\dagger d_{0\sigma} + h.c.)$ describes the coupling between the QD₀ and the leads, where $\mathcal{V}_{k\alpha\sigma}$ denotes the hopping amplitude between QD₀ of the central region and state k of lead $\alpha = L/R$. The term \mathcal{H}_{dot} describes the central region made of three QD in a triangular shape which we model as follows

$$\begin{aligned} \mathcal{H}_{dot} = & \sum_{j=0,\sigma}^2 \epsilon_{j\sigma} d_{j\sigma}^\dagger d_{j\sigma} + t_1 \sum_{\sigma} (d_{0\sigma}^\dagger d_{1\sigma} + h.c.) \\ & + t_2 \sum_{\sigma} (d_{0\sigma}^\dagger d_{2\sigma} + h.c.) + t_3 \sum_{\sigma} (d_{1\sigma}^\dagger d_{3\sigma} + h.c.) \\ & + U n_{\sigma\uparrow} n_{\sigma\downarrow}, \end{aligned} \quad (2)$$

where $d_{j\sigma}^\dagger$ ($d_{j\sigma}$) are fermion creation (annihilation) operators at QD_j, U is the Coulomb-interaction and the number operator is given by $n_{0\sigma} = d_{0\sigma}^\dagger d_{0\sigma}$ with spin σ at QD₀.

Electron current can be measured through the time evolution of the expectation value of electron occupation in one of the leads $I_\alpha = -e \frac{d}{dt} \langle n_\alpha \rangle$, where $n_\alpha = \sum_{k\alpha\sigma} d_{k\alpha\sigma}^\dagger d_{k\alpha\sigma}$. Since the total density commutes with the Hamiltonian Eq. (1), the current conservation requires that in steady-state to have $\sum_\alpha I_\alpha = 0$. Hence the current flowing through the system is considered $I \equiv I_L = -I_R$. Utilizing the Keldysh formalism³⁶ current through the interacting quantum dot reads as follows

$$I = -\frac{e}{\pi\hbar} \int dE \sum_{\sigma} \frac{\Gamma_L \Gamma_R}{\Gamma} \mathbf{Im} G_{\sigma,\sigma}^r(E) [f_L(E) - f_R(E)], \quad (3)$$

where $G_{\sigma,\sigma}^r(E)$ is the model retarded Green function in the presence of both coupling to the continuum

states and electron-electron interactions. $\Gamma_\alpha(E) = 2\pi\rho_\alpha(E)|\mathcal{V}_{\alpha\sigma}(E)|$ represents the level broadening due to coupling to the leads (with total line width $\Gamma = \sum_\alpha \Gamma_\alpha$, and the density of states $\rho_\alpha = \sum_k \delta(E - \epsilon_{\alpha k})$ in the α lead). We consider wide band limit in this paper, so $\Gamma_\alpha(E) \equiv \Gamma_\alpha$. We also consider the density of states and the probability of tunneling independent of spin (non-magnetic electrodes). $f_\alpha(E) = [1 + \exp(E - \mu_\alpha)/(k_B T_\alpha)]^{-1}$ is the Fermi-Dirac function for lead α with electrochemical potential $\mu_\alpha = E_F + eV_\alpha$ and temperature $T_\alpha = T + \theta_\alpha$ (where E_F is the Fermi energy and T is the background temperature).

As stated before, we adapt the equation-of-motion technique and restrict it to the Coulomb-blockade regime where two energies scale of the model, namely $k_B T$ and Γ are much smaller than the U . Within such a restriction, ignoring the complex cotunneling process and working in temperature $T > T_K$ larger than the Kondo temperature, the equation-of-motion approach generates a good description of the transport properties of strongly interacting quantum dots.

Retarded green function $G^r(\tau, 0)$ of two fermionic operators A and B , and the corresponding equation of motion in energy domain given as

$$G_{A,B}^r(\tau, 0) = \ll A, B \gg_\tau^r = -i\theta(\tau) \langle \{A(\tau), B(0)\} \rangle, \quad (4)$$

$$(\epsilon + i0^+) \ll A, B \gg_\epsilon^r + \ll [H, A], B \gg_\epsilon^r = \langle \{A, B\} \rangle$$

where H is the total Hamiltonian Eq. (1), and 0^+ is an infinitesimal real number. For the sake of simplicity, in the following we omit index r and 0^+ . Then for QD₀ we have

$$\epsilon \ll d_{0\sigma}, d_{0\sigma}^\dagger \gg = \langle \{d_{0\sigma}, d_{0\sigma}^\dagger\} \rangle - \ll [H, d_{0\sigma}], d_{0\sigma}^\dagger \gg \quad (5)$$

by inserting Eq. (1) into the above equation, we get

$$\begin{aligned} (\epsilon - \epsilon_{0\sigma}) \ll d_{0\sigma}, d_{0\sigma}^\dagger \gg = & 1 + U \ll d_{0\sigma} n_{0,\bar{\sigma}}, d_{0\sigma}^\dagger \gg \\ & + \sum_{\alpha k\sigma} \mathcal{V}_{k\alpha\sigma}^* \ll c_{k\alpha\sigma}, d_{0\sigma}^\dagger \gg + t_1 \ll d_{1\sigma}, d_{0\sigma}^\dagger \gg \\ & + t_2 \ll d_{2\sigma}, d_{0\sigma}^\dagger \gg \end{aligned} \quad (6)$$

where

$$\ll c_{k\alpha\sigma}, d_{0\sigma}^\dagger \gg = \frac{\mathcal{V}_{k\alpha\sigma}}{\epsilon - \epsilon_{k\alpha}} \ll d_{0\sigma}, d_{0\sigma}^\dagger \gg \quad (7)$$

and to find $\ll d_{1(2)\sigma}, d_{0\sigma}^\dagger \gg$, we only need to use Eq. (4), then we have

$$\begin{aligned} \ll d_{1\sigma}, d_{0\sigma}^\dagger \gg = & \frac{t_1^*}{\epsilon - \epsilon_{1\sigma}} \ll d_{0\sigma}, d_{0\sigma}^\dagger \gg \quad (8) \\ & + \frac{t_3 t_2^*}{(\epsilon - \epsilon_{1\sigma})(\epsilon - \epsilon_{2\sigma})} \ll d_{0\sigma}, d_{0\sigma}^\dagger \gg \\ & + \frac{|t_3|^2}{(\epsilon - \epsilon_{1\sigma})(\epsilon - \epsilon_{2\sigma})} \ll d_{1\sigma}, d_{0\sigma}^\dagger \gg, \end{aligned}$$

$$\begin{aligned}
\ll d_{2\sigma}, d_{0\sigma}^\dagger \gg &= \frac{t_2^*}{\epsilon - \epsilon_{1(2)\sigma}} \ll d_{0\sigma}, d_{0\sigma}^\dagger \gg \quad (9) \\
&+ \frac{t_3^* t_1^*}{(\epsilon - \epsilon_{1\sigma})(\epsilon - \epsilon_{2\sigma})} \ll d_{0\sigma}, d_{0\sigma}^\dagger \gg \\
&+ \frac{|t_3|^2}{(\epsilon - \epsilon_{1\sigma})(\epsilon - \epsilon_{2\sigma})} \ll d_{2\sigma}, d_{0\sigma}^\dagger \gg,
\end{aligned}$$

with more simplification and by defining two new parameters

$$\begin{aligned}
\Sigma_1 &= \frac{t_1^*(\epsilon - \epsilon_{2\sigma}) + t_3 t_2^*}{(\epsilon - \epsilon_{1\sigma})(\epsilon - \epsilon_{2\sigma}) - |t_3|^2} \\
\Sigma_2 &= \frac{t_1^*(\epsilon - \epsilon_{2\sigma}) + t_3 t_2^*}{(\epsilon - \epsilon_{1\sigma})(\epsilon - \epsilon_{2\sigma}) - |t_3|^2},
\end{aligned}$$

we find a compact form

$$\ll d_{1(2)\sigma}, d_{0\sigma}^\dagger \gg = \Sigma_{1(2)} \ll d_{0\sigma}, d_{0\sigma}^\dagger \gg,$$

where by substitution it and Eq. (7) into Eq. (6) we arrive

$$\begin{aligned}
(\epsilon - \epsilon_{0\sigma}) \ll d_{0\sigma}, d_{0\sigma}^\dagger \gg &= 1 + U \ll d_{0\sigma} n_{0,\bar{\sigma}}, d_{0\sigma}^\dagger \gg \\
&+ \left(\sum_{\alpha k \sigma} \frac{|\mathcal{V}_{k\alpha\sigma}|^2}{\epsilon - \epsilon_{\alpha k \sigma}} + \sum_{i=1,2} t_i \Sigma_i \right) \ll d_{0\sigma}, d_{0\sigma}^\dagger \gg \quad (10)
\end{aligned}$$

with recasting and operating the wide-band approximation $\Sigma_0 = \sum_{\alpha k \sigma} \frac{|\mathcal{V}_{k\alpha\sigma}|^2}{\epsilon - \epsilon_{\alpha k}} \simeq \frac{\Gamma}{\pi} \ln \left| \frac{D+\epsilon}{D-\epsilon} \right| - i \frac{\Gamma}{2}$ the Eq. (10) can be read as

$$\begin{aligned}
\left(\epsilon - \epsilon_{0\sigma} - \Sigma_0 - \sum_{i=1,2} t_i \Sigma_i \right) \ll d_{0\sigma}, d_{0\sigma}^\dagger \gg &= \\
1 + U \ll d_{0\sigma} n_{0,\bar{\sigma}}, d_{0\sigma}^\dagger \gg &\quad (11)
\end{aligned}$$

In the above fomula still we need $\ll d_{0\sigma} n_{0,\bar{\sigma}}, d_{0\sigma}^\dagger \gg$. Using Eq. (4) and ignoring higher-order correlation terms, we find

$$\begin{aligned}
(\epsilon - \epsilon_{0\sigma} - U) \ll d_{0\sigma} n_{0,\bar{\sigma}}, d_{0\sigma}^\dagger \gg &\quad (12) \\
&- \sum_{k\alpha\sigma} \mathcal{V}_{k\alpha\sigma} \ll c_{k\alpha\sigma} n_{0,\bar{\sigma}}, d_{0\sigma}^\dagger \gg \\
&- \sum_{i=1,2} t_i \ll d_{i\sigma} n_{0,\bar{\sigma}}, d_{0\sigma}^\dagger \gg \approx \langle n_{0\bar{\sigma}} \rangle,
\end{aligned}$$

where

$$\begin{aligned}
\ll c_{k\alpha\sigma} n_{0,\bar{\sigma}}, d_{0\sigma}^\dagger \gg &= \sum_{k\alpha\sigma} \frac{\mathcal{V}_{k\alpha\sigma}}{\epsilon - \epsilon_{k\alpha\sigma}} \ll d_{0\sigma} n_{0,\bar{\sigma}}, d_{0\sigma}^\dagger \gg \\
\ll d_{i\sigma} n_{0,\bar{\sigma}}, d_{0\sigma}^\dagger \gg &= \Sigma_i \ll d_{0\sigma} n_{0,\bar{\sigma}}, d_{0\sigma}^\dagger \gg, \quad (13)
\end{aligned}$$

inserting Eq. (13) into Eq. (12), we arrive

$$\ll d_{0\sigma} n_{0,\bar{\sigma}}, d_{0\sigma}^\dagger \gg = \frac{\langle n_{0\bar{\sigma}} \rangle}{\epsilon - \epsilon_{0\sigma} - \Sigma_0 - \sum_{i=1,2} t_i \Sigma_i - U} \quad (14)$$

wrapping all, we end a closed-form Green's function for QD₀ as

$$\begin{aligned}
G_{\sigma,\sigma}^r(E) &= \ll d_{0\sigma}, d_{0\sigma}^\dagger \gg \\
&= \frac{1 - \langle n_{0\bar{\sigma}} \rangle}{\epsilon - \epsilon_{0\sigma} - \Sigma_0 - \sum_{i=1,2} \Sigma'_i} \\
&= \frac{\langle n_{0\bar{\sigma}} \rangle}{\epsilon - \epsilon_{0\sigma} - \Sigma_0 - \sum_{i=1,2} \Sigma'_i - U} \quad (15)
\end{aligned}$$

where $\Sigma'_i = t_i \Sigma_i$, ($i = 1, 2$). This shows $G_{\sigma,\sigma}^r(E)$ depends on the dot occupation for reversed spin $\bar{\sigma}$, $\langle n_{\sigma} \rangle = \frac{1}{2\pi i} \int dE G_{\sigma,\sigma}^<(E)$. Using the Keldysh equation for lesser green function $G_{\sigma,\sigma}^<(E) = i[\Gamma_L f_L(E) + \Gamma_R f_R(E)] |G_{\sigma,\sigma}^r(E)|^1$, and adapting the self-consistent approach we close the system of equations. Analogous to charge current, the heat current is derived from

$$\begin{aligned}
J_\alpha &= \frac{d \left\langle \sum_{k\alpha\sigma} d_{k\alpha\sigma}^\dagger d_{k\alpha\sigma} \right\rangle}{dt} \quad (16) \\
&= \sum_{\sigma} \frac{\Gamma_L \Gamma_R}{\pi \hbar \Gamma} \int dE (\mu_\alpha - E) \mathbf{Im} G_{\sigma,\sigma}^r(E) [f_L(E) - f_R(E)]
\end{aligned}$$

which satisfies the Joule law $J_R + J_L = -IV$.

III. RESULTS AND DISCUSSION

Now, we present the results obtained based on the formulation of the previous section. We select the level broadening of QD₀ due to coupling to the leads $\Gamma_L = \Gamma_R = \Gamma_0$ as a unit of energy. Interested in the Coulomb-blockade regime we appoint background temperature energy and the Coulomb interaction as $k_B T = 0.1\Gamma_0$ and $U = 10\Gamma_0$, respectively. We also consider all hopping integrals equal as $t_i = \Gamma_0$, ($i = 1, 2, 3$).

Figs. 2(a) and (b) display the average occupation number and electric current of the QD₀, respectively, in terms of voltage bias for different QD₀'s energy values in the absence of temperature gradient ($\theta = 0$). The bias voltage applied in a symmetric way to the junction ($\mu_L = -\mu_R = eV/2$), and impose $E_F = 0$ as the reference energy point. As it is clear from Fig. 2(b), for zero bias voltage, when the dot energy level resonates with Fermi energy, the setup acts as an ohmic junction. With increasing voltage, the current shows a step behavior which is a characteristic of the quantum junction and is in accordance with the phenomenological models related to the Coulomb-blockade^{37,38}. The increase in current occurs when the dot energies of the system are in line with the chemical potential of the electrodes. Furthermore, Fig. 2(a) displays the level occupation depends strongly on dot level and bias voltage. In a single quantum dot junction, at the particle-hole symmetry point $\epsilon_0 = -U/2$, the occupation is voltage independent¹⁸. It happens since the exchanging $d \rightarrow d^\dagger$ leaves the Hamiltonian of model unaffected. In the triangle quantum dot model defined

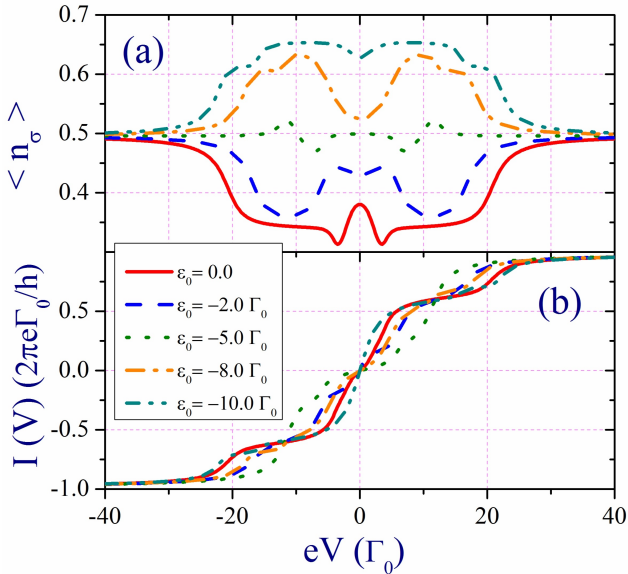


FIG. 2. (color online) (Color online) Panels (a) and (b) show average of occupation number and electrical current of QD_0 as function of bias voltage, respectively. Lines correspond to different dot level. Note, we consider a pure voltage-driven process by setting $\theta = 0$.

in Eq. (1), particle-hole symmetry is spoiled, as it can be seen from result of $\epsilon_0 = -5\Gamma_0$, and shown in a dotted-line on Fig. 2(a).

Fig. 3 displays the average occupation number and heat current of QD_0 in terms of the temperature gradient between the two right and left electrodes for different dot energy levels with zero applied bias. Note that in order to have temperature gradient $\theta = \theta_L - \theta_R$, without loss of generality, we set $\theta_L = \theta$ and $\theta_R = 0$. In the presence of the temperature gradient, the energy levels renormalize themselves. In this case, there is a displacement in the location of the energy levels of the junction, which can cause a fundamental change in the intensity of electron transport through the junction. Electron flow occurs when the renormalized energy level of the system is close to the chemical potential of the electrodes. The intensity of this flow determines the magnitude of the thermal current.

For negative (positive) current, the charge carriers are holes (electrons). The results show that the direction of the charge carriers depends on the energy of the QD_0 . For the energy $\epsilon_0 \neq -U/2$, the heat current are not zero because the electronic density of states around the Fermi energy is asymmetric. To have a better insight of the charge carrier transport process, in Fig. 4 we illustrate the heat currents in terms of the temperature difference between the right and left electrodes for dot energy $\epsilon_0 = 0$. Three left panels (a), (b), and (c) depict a schematic cartoon of the thermally driven transport process through the junction corresponding to points in-

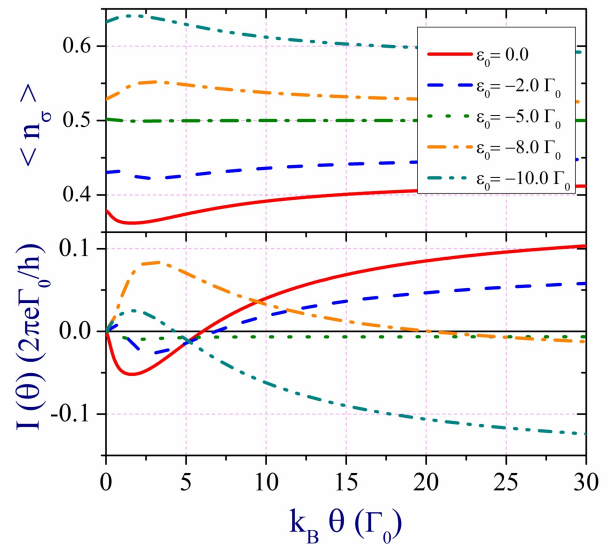


FIG. 3. (color online) (Colore online) Pannels (a) and (b) show average of occupation number and electrical current of QD_0 as function of temperature gradient, respectively. Lines correspond to different dot level. Here, we consider a pure temperature-driven process by setting $V = 0$.

indicated by A, B, and C in the right panels, respectively. At $\theta = 0$ heat current is zero, and with increasing θ , the Fermi distribution loses its step function form. The direction of charge flow depends on the dot energy level and the density of state around the Fermi energy (see the horizontal dashed line on the Fig. 4).

At point **A**, due to the ordering of energy levels and the density of energy states, it is evident that the contribution of holes in the charge flow is greater than the contribution of electrons, and therefore the heat current is negative. With increasing θ , Fermi distribution extends its tail to higher energies and then make it possible to have more electrons get excited through the junction. By raising the temperature difference more, total heat current again becomes zero, which indicates the balance between the flow of electrons and holes in both directions (see point **B** on the Fig. 4). Since the number of energy levels available at $E > 0$ and dot level ϵ_0 are bigger, increasing θ leads to higher electrons flow contribution to the total heat current and make it positive, see point **C** on the Fig. 4.

Fig. 5 shows the thermovoltage (V_{th}) versus the temperature difference between the right and left electrodes for different QDs energies. The thermovoltage or Seebeck voltage is obtained by imposing the open-circuit condition $I(V_{\text{th}}, \theta) = 0$, which we extract numerically.

At very low θ s, thermovoltage is a linear function in terms of temperature that can be positive (for electrons) or negative (for holes) depending on the nature of the charge carriers. While at higher θ , V_{th} shows a nonlinear

trend. With raising θ , V_{th} 's absolute magnitude increases and gets an extremum. With increasing more the temperature gradient, V_{th} decreases and for a temperature $\theta = \theta_0$, V_{th} becomes zero, and V_{th} changes the sign or $\theta > \theta_0$.

This result is in agreement with experiments on semiconductor quantum dots³¹. The change of the V_{th} sign can be justified as follows: The chemical potential of the electrodes at zero bias voltage is zero. If electrons are the charge carriers, the temperature difference at the electrodes causes the electron to flow from the left electrode (hot) to the right electrode (cold). To reduce this heat current, a negative thermovoltage appears, which grows with increasing θ . Although, with raising θ , the step of the Fermi distribution of the left (hot) electrode is somewhat smoothed such that the hole carries now flow easily to the right electrode. At temperature gradient, θ_0 , these flows of electrons and holes become equal and suppress each other leading to a zero heat current. We notice that for the triangle quantum dot setup, considered in this work, at dot energy level $\epsilon_0 = -U/2$, thermovoltage is always nonzero and positive, unlike the single quantum dot setup, which is related to the particle-hole symmetry broken.

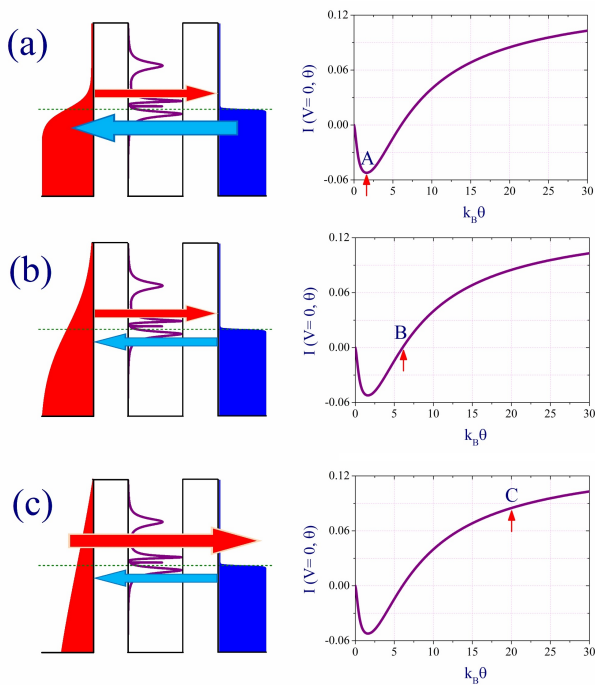


FIG. 4. (Color online) Right panels show a heat current as a function of temperature gradient θ at dot level $\epsilon = 0$. Left panels draw a schematic cartoon of the energy diagram of the transport process through the junction, for three points shown on the heat current plots.

Materials that have good thermoelectric properties can transform heat into electricity, which is called the See-

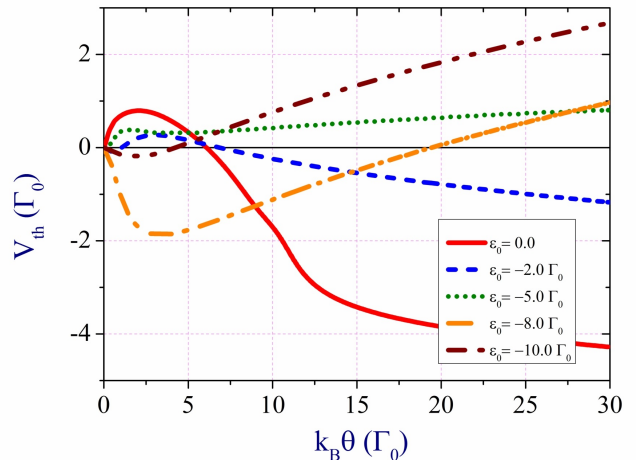


FIG. 5. (Color online) Thermovoltage diagram V_{th} in terms of temperature difference between the right and left electrodes for different energy level of the QD₀.

beck effect. The Peltier effect is the opposite of the Seebeck effect²⁹. An electric current that passes through the junction of two substances emits or absorbs heat per unit time at the junction to balance the chemical potential difference between the two substances. The effect of the Peltier, which describes the reversible heat, depends on the direction of the current and, unlike Joule heating, which is irreversible, can be used to cool electrical devices. Recent experimental results indicate that the heat generated at atoms of atomic dimensions shows asymmetric rectification in terms of voltage^{39–41}. These results are very interesting because while the effects of rectification on the subject of electricity are well known, little is known about how power is lost in mesoscopic conductors under bias voltage.

The linear part of the rectified heat is obtained through the linear response of the Peltier coefficient. Therefore, the power dissipation for positive bias voltage can be greater or less than negative bias voltage, which depends on the placement of resonant energy levels above or below the Fermi energy. Fig.6 shows the heat flow in terms of bias voltage for different amounts of positional energy. As can be seen, for all quantities of dot level positions, the heat flow is an asymmetric function in terms of the voltage sign. In addition, the nonlinear behavioral heat flow indicates that the effect of higher orders is dominant. It is interesting to note that for all the QD's energy level positions, the heat flow can be positive or negative (reversible heat) indicating an unusual heat flow for non-zero voltage (whose value depends on the dot level positions) becomes zero (see the inset Fig.6(a)).

In Fig. 6(b) we depict the rectification factor $J(V) - J(-V)$ as a function of applied voltage for different dot level positions. For all quantities of dot levels, the sign of the rectifier coefficient changes. For positive values of

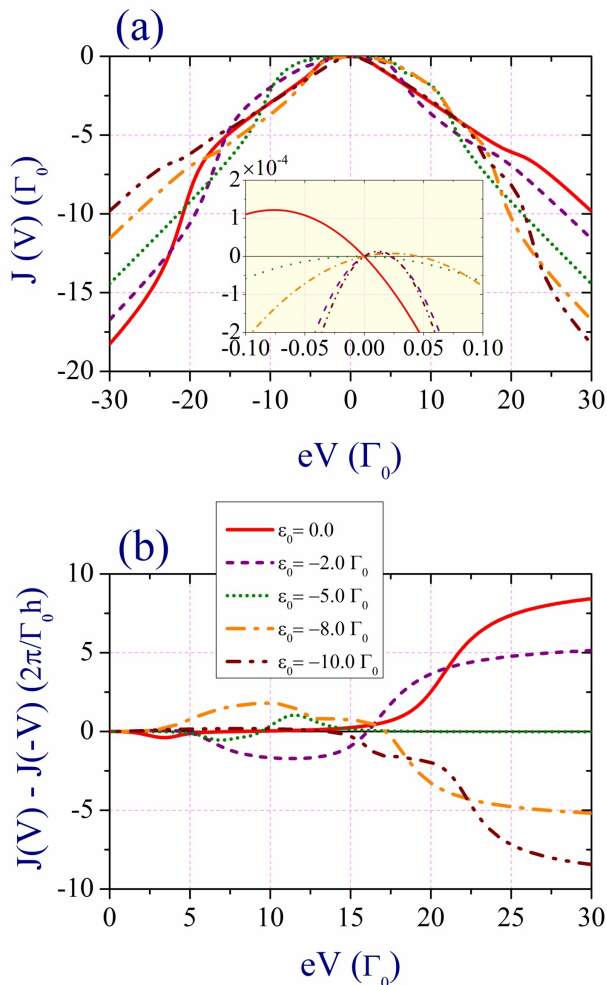


FIG. 6. (Color online) (a) Heat current and (b) the rectification factor as a function of applied voltage in the isothermal case $\theta = 0$. Inset: Detail of the dissipated power around zero voltage.

the rectification factor, the heat dissipation for $V > 0$ is higher than the heat dissipation in the $V < 0$. At high voltages, R tends to a constant value, because in this range, the Fermi function of the left electrode tends to number one and the Fermi function of the right electrode tends to zero, and the energy flow becomes voltage-independent.

IV. CONCLUSIONS

In this paper, we theoretically investigate the voltage, temperature current and heat dissipation through a triangular quantum dot (QD) attached to the metal electrodes. Calculations were performed using a combination of the non-equilibrium Green function and the equation of motion method in the Coulomb blockade regime. The results show that at the triangular quantum dot, the voltage and temperature current behave nonlinear, and their magnitude and sign depend on factors such as the dot energy level and the hopping parameter between QDs. Based on self-consistent calculations, we showed that the heat current is a nonlinear function concerning the applied voltage. Moreover, the heat current responding the change of the applied voltage and for all quantities of dot energy levels is an asymmetric function. This feature is unlike the single quantum dot connected to metallic electrodes as reported by Aothur in Ref.¹⁸. We hope the results presented in this work, could shed light on determining the performance of nanoscale electronic devices (in which nonlinear effects are important) to control heat dissipations.

V. ACKNOWLEDGEMENT

J. V gratefully acknowledge support from Deutsche Forschungsgemeinschaft (DFG) KE-807/22-1.

* a.ahmadifouladi@iausari.ac

† j.vahedi@jacobs-university.de

¹ Björn Sothmann, Rafael Sánchez, and Andrew N Jordan, “Thermoelectric energy harvesting with quantum dots,” *Nanotechnology* **26**, 032001 (2014).

² Jeffrey J. Urban, “Prospects for thermoelectricity in quantum dot hybrid arrays,” *Nature Nanotechnology* **10**, 997–1001 (2015).

³ Paolo Andrea Erdman, Francesco Mazza, Riccardo Bosio, Giuliano Benenti, Rosario Fazio, and Fabio Taddei, “Thermoelectric properties of an interacting quantum dot based heat engine,” *Phys. Rev. B* **95**, 245432 (2017).

⁴ Vincent Talbo, Jérôme Saint-Martin, Sylvie Retailleau, and Philippe Dollfus, “Non-linear effects and thermoelectric efficiency of quantum dot-based single-electron transistors,” *Scientific Reports* **7** (2017), 10.1038/s41598-017-14009-4.

⁵ Bitan De and Bhaskaran Muralidharan, “Non-linear phonon peltier effect in dissipative quantum dot systems,” *Scientific Reports* **8** (2018), 10.1038/s41598-018-23402-6.

⁶ G Menichetti, G Grosso, and G Pastori Parravicini, “Analytic treatment of the thermoelectric properties for two coupled quantum dots threaded by magnetic fields,” *Journal of Physics Communications* **2**, 055026 (2018).

⁷ Gaomin Tang, Lei Zhang, and Jian Wang, “Thermal rectification in a double quantum dots system with a polaron effect,” *Phys. Rev. B* **97**, 224311 (2018).

⁸ Maria Florencia Ludovico and Massimo Capone, “Enhanced performance of a quantum-dot-based nanomotor due to coulomb interactions,” *Phys. Rev. B* **98**, 235409 (2018).

⁹ Artis Svilans, Martin Josefsson, Adam M. Burke, Sofia Fahlvik, Claes Thelander, Heiner Linke, and Martin Leijnse, “Thermoelectric characterization of the kondo resonance in nanowire quantum dots,” *Phys. Rev. Lett.* **121**,

- 206801 (2018).
- 10 Martin Josefsson, Artis Svilans, Adam M. Burke, Eric A. Hoffmann, Sofia Fahlvik, Claes Thelander, Martin Leijnse, and Heiner Linke, “A quantum-dot heat engine operating close to the thermodynamic efficiency limits,” *Nature Nanotechnology* **13**, 920–924 (2018).
 - 11 Martin Josefsson, Artis Svilans, Heiner Linke, and Martin Leijnse, “Optimal power and efficiency of single quantum dot heat engines: Theory and experiment,” *Phys. Rev. B* **99**, 235432 (2019).
 - 12 Feng Chi, Zhen-Guo Fu, Jia Liu, Ke-Man Li, Zhigang Wang, and Ping Zhang, “Thermoelectric effect in a correlated quantum dot side-coupled to majorana bound states,” *Nanoscale Research Letters* **15** (2020), 10.1186/s11671-020-03307-y.
 - 13 Federico D. Ribetto, Raúl A. Bustos-Marín, and Hernán L. Calvo, “Role of coherence in quantum-dot-based nanomachines within the coulomb blockade regime,” *Phys. Rev. B* **103**, 155435 (2021).
 - 14 Kum Hyok Jong, Song Mi Ri, and Chol Won Ri, “Parametric study for optimal performance of coulomb-coupled quantum dots,” *Journal of Physics: Condensed Matter* **33**, 375302 (2021).
 - 15 Sagnik Banerjee and Aniket Singha, “A non-local cryogenic thermometer based on coulomb-coupled systems,” *Journal of Applied Physics* **129**, 114901 (2021).
 - 16 Sven Dorsch, Artis Svilans, Martin Josefsson, Bahareh Goldozian, Mukesh Kumar, Claes Thelander, Andreas Wacker, and Adam Burke, “Heat driven transport in serial double quantum dot devices,” *Nano Letters* **21**, 988–994 (2021).
 - 17 Natalya A Zimbovskaya, “Large enhancement of thermoelectric effects in multiple quantum dots in a serial configuration due to coulomb interactions,” *Journal of Physics: Condensed Matter* **34**, 255302 (2022).
 - 18 Miguel A. Sierra and David Sánchez, “Strongly nonlinear thermovoltage and heat dissipation in interacting quantum dots,” *Phys. Rev. B* **90**, 115313 (2014).
 - 19 Natalya A. Zimbovskaya, “The effect of coulomb interactions on nonlinear thermovoltage and thermocurrent in quantum dots,” *The Journal of Chemical Physics* **142**, 244310 (2015).
 - 20 Miguel A. Sierra and David Sánchez, “Nonlinear heat conduction in coulomb-blockaded quantum dots,” *Materials Today: Proceedings* **2**, 483–490 (2015).
 - 21 Natalya A Zimbovskaya, “Nonlinear thermoelectric transport in single-molecule junctions: the effect of electron–phonon interactions,” *Journal of Physics: Condensed Matter* **28**, 295301 (2016).
 - 22 David Sánchez and Rosa López, “Nonlinear phenomena in quantum thermoelectrics and heat,” *Comptes Rendus Physique* **17**, 1060–1071 (2016).
 - 23 Artis Svilans, Adam M. Burke, Sofia Fahlvik Svensson, Martin Leijnse, and Heiner Linke, “Nonlinear thermoelectric response due to energy-dependent transport properties of a quantum dot,” *Physica E: Low-dimensional Systems and Nanostructures* **82**, 34–38 (2016).
 - 24 G. Gomes-Silva, P. A. Orellana, and E. V. Anda, “Enhancement of the thermoelectric efficiency in a t-shaped quantum dot system in the linear and nonlinear regimes,” *Journal of Applied Physics* **123**, 085706 (2018).
 - 25 Zahra Sartipi, Amir Hayati, and Javad Vahedi, “Thermoelectric efficiency in three-terminal graphene nanojunctions,” *The Journal of Chemical Physics* **149**, 114103 (2018).
 - 26 Z. Sartipi and J. Vahedi, “Enhancing thermoelectric properties through a three-terminal benzene molecule,” *The Journal of Chemical Physics* **148**, 174302 (2018).
 - 27 P. A. Erdman, J. T. Peltonen, B. Bhandari, B. Dutta, H. Courtois, R. Fazio, F. Taddei, and J. P. Pekola, “Nonlinear thermovoltage in a single-electron transistor,” *Phys. Rev. B* **99**, 165405 (2019).
 - 28 Nobuhiko Taniguchi, “Quantum control of nonlinear thermoelectricity at the nanoscale,” *Phys. Rev. B* **101**, 115404 (2020).
 - 29 H. Julian Goldsmid, *Introduction to Thermoelectricity* (Springer Berlin Heidelberg, 2010).
 - 30 A. A. M. Staring, L. W. Molenkamp, B. W. Alphenaar, H. van Houten, O. J. A. Buyk, M. A. A. Mabesoone, C. W. J. Beenakker, and C. T. Foxon, “Coulomb-blockade oscillations in the thermopower of a quantum dot,” *Europhysics Letters (EPL)* **22**, 57–62 (1993).
 - 31 S. Fahlvik Svensson, E. A. Hoffmann, N. Nakpathomkun, P. M. Wu, H. Q. Xu, H. A. Nilsson, D. Sánchez, V. Kashcheyevs, and H. Linke, “Nonlinear thermovoltage and thermocurrent in quantum dots,” *New Journal of Physics* **15**, 105011 (2013).
 - 32 M. Wierzbicki and R. Świrkowicz, “Electric and thermoelectric phenomena in a multilevel quantum dot attached to ferromagnetic electrodes,” *Phys. Rev. B* **82**, 165334 (2010).
 - 33 X. Zianni, “Coulomb oscillations in the electron thermal conductance of a dot in the linear regime,” *Phys. Rev. B* **75**, 045344 (2007).
 - 34 Natalya A Zimbovskaya, “Charge and heat current rectification by a double-dot system within the coulomb blockade regime,” *Journal of Physics: Condensed Matter* **32**, 325302 (2020).
 - 35 Miguel A. Sierra, M. Saiz-Bretín, F. Domínguez-Adame, and David Sánchez, “Interactions and thermoelectric effects in a parallel-coupled double quantum dot,” *Phys. Rev. B* **93**, 235452 (2016).
 - 36 Yigal Meir and Ned S. Wingreen, “Landauer formula for the current through an interacting electron region,” *Phys. Rev. Lett.* **68**, 2512–2515 (1992).
 - 37 Yigal Meir, Ned S. Wingreen, and Patrick A. Lee, “Transport through a strongly interacting electron system: Theory of periodic conductance oscillations,” *Phys. Rev. Lett.* **66**, 3048–3051 (1991).
 - 38 C. W. J. Beenakker, “Theory of coulomb-blockade oscillations in the conductance of a quantum dot,” *Phys. Rev. B* **44**, 1646–1656 (1991).
 - 39 Woochul Lee, Kyeongtae Kim, Wonho Jeong, Linda Angela Zotti, Fabian Pauly, Juan Carlos Cuevas, and Pramod Reddy, “Heat dissipation in atomic-scale junctions,” *Nature* **498**, 209–212 (2013).
 - 40 L. A. Zotti, M. Bürkle, F. Pauly, W. Lee, K. Kim, W. Jeong, Y. Asai, P. Reddy, and J. C. Cuevas, “Heat dissipation and its relation to thermopower in single-molecule junctions,” *New Journal of Physics* **16**, 015004 (2014).
 - 41 Yaghoob Naimi and Javad Vahedi, “Heat dissipation and its relation to molecular orbital energies in single-molecule junctions,” *physica status solidi (b)* **252**, 2714–2722 (2015).